KERNFORSCHUNGSANLAGE JÜLICH GmbH

Institut für Plasmaphysik
Association EURATOM-KFA

ENHANCED SMALL SCALE TURBULENCE OSCILLATIONS CORRELATED TO SAWTOOTH RELAXATIONS IN THE TEXTOR TOKAMAK

by
A. Rogister, G. Hasselberg, A. Kaleck,
A. Boileau, H.W.H. Van Andel and M. von Hellermann

Jül-2025
November 1985
ISSN 0366-0885

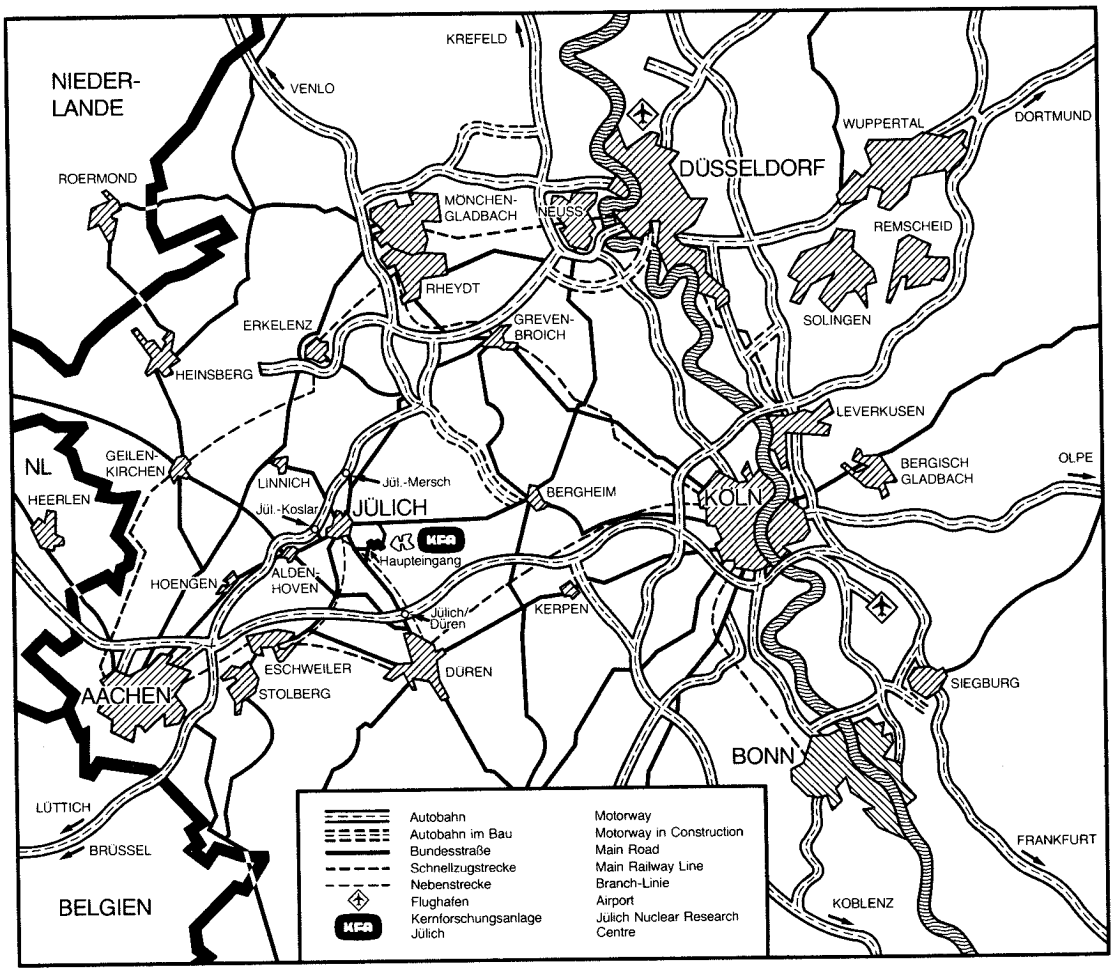

Als Manuskript gedruckt

Berichte der Kernforschungsanlage Jülich – Nr. 2025
Institut für Plasmaphysik, Association EURATOM-KFA Jül-2025

Zu beziehen durch: ZENTRALBIBLIOTHEK der Kernforschungsanlage Jülich GmbH
Postfach 1913 · D-5170 Jülich (Bundesrepublik Deutschland)
Telefon: 02461/610 · Telex: 833556-0 kf d

ENHANCED SMALL SCALE TURBULENCE OSCILLATIONS CORRELATED TO SAWTOOTH RELAXATIONS IN THE TEXTOR TOKAMAK

by
A. Rogister, G. Hasselberg, A. Kaleck,
A. Boileau, H.W.H. Van Andel and M. von Hellermann

ENHANCED SMALL SCALE TURBULENCE OSCILLATIONS CORRELATED TO SAWTOOTH RELAXATIONS IN THE TEXTOR TOKAMAK.

A. Rogister, G. Hasselberg, A. Kaleck,

Institut für Plasmaphysik der Kernforschungsanlage Jülich GmbH, Association EURATOM/KFA, 5170 Jülich, Postfach 1913, FRG.

A. Boileau*, H.W.H. Van Andel**

Dêpartement de Physique, Universitê de Montrêal, C.P. 6128, Montréal H3C 3J7, Canada.

M. von Hellermann+

Universität Essen, Fachbereich Physik, Postfach 6843, Essen 4300, FRG.

ABSTRACT.

A periodic enhancement of the microturbulence level by sawtooth relaxations has been detected by CO_2 laser forward scattering in the TEXTOR tokamak. This feature is reproduced quantitatively by a heat transport code in which the anomalous electron transport coefficient is calculated self consistently following a theoretical model of the saturation of the dissipative trapped electron instability. The code also predicts a strong modulation of the heat flux throughout the whole plasma and a strong "profile consistency" as continuous temperature measurements have demonstrated. A simple interpretation of these results is given. Calculated global plasma parameters, such as the energy confinement time and the loop voltage, are in good agreement with the measured values.

* Present address: INRS-ENERGIE, 1650 Montêe Ste-Julie, CP 1020, Varennes, Quêbec, Canada JOL 2PO

** The King's College, 10766 97th Street, Edmonton, Alberta, Canada T5H 2M1

+ JET Joint Undertaking, Abingdon, Oxfordshire, OX 14 3EA

1. INTRODUCTION.

Microturbulence ($k_\perp a_i \sim 1$; a_i = ion Larmor radius) is a distinct feature of tokamak plasmas /1-9/ as many laser coherent scattering experiments have reported. Its spectral distribution can be measured and/or calculated from suitable nonlinear theories describing the saturation of the associated low frequency instabilities ($\omega \ll \Omega_i$ = ion gyrofrequency). This spectral distribution yields, by a simple calculation, the "anomalous" transport coefficients of heat, base particles, and impurities. Different saturation mechanisms have been proposed leading not only to different transport rates, but also to distinct pictures of transport /10-14/. We consider here the implications of the theory developed in References /13, 14/.

This model, in which nonlinear saturation occurs through Compton and induced scattering (respectively diffraction by the bare particles and by their shielding cloud) predicts both an energy cascade towards long wavelengths (if $k_\perp a_i < 1$) or short wavelengths (if $k_\perp a_i > 1$), and a direct energy transfer from the low to the high mode numbers of the spectrum characterized by equal frequencies. Associated transport calculations further showed that the high mode numbers provide the dominant contribution to the heat conduction and the particle diffusion coefficients while the low mode numbers account for most of the density autocorrelation. A crucial result of the theoretical investigation was the discovery that both the transport and the turbulence level are very sensitive functions of the linear growth rate of the instability, and thereby of the temperature T_e, the density N, their gradients, and the shear parameter $\hat{\sigma} = d\ln q / d\ln r$ /15/.

This sensitivity, if verified by the experiment, suggests that both the transport coefficients and the turbulence level are actually modulated by the sawtooth relaxations of the hot plasma core since the expelled energy pulse modifies locally the temperature, the density, etc...., as it propagates towards the plasma edge.

The pulse thus influences its own transport rate, somewhat as the steepening of a collisionless shock wave interferes with its own dissipation rate /16/. In particular, the small time delays required to arrive at the limiter or the neutralizer plate /17,18/ could be explained by the formula

$$u_p \approx -\frac{2}{3}\,\frac{1}{r}\,\frac{\partial}{\partial r}\,r K_e$$

since the propagating front is expected to be localized (u_p is the propagation velocity of the pulse and K_e the heat conduction coefficient).

Before concluding this section, we recall the shortcomings of the theory. It relies, at present, on the weak turbulence approach - it is thus unable to explain the observed line broadening - and on a temperature ratio ($T_i/T_e \ll 1$) expansion. Both approximations, introduced to simplify extremely complicated equations, are inadequate for a fusion plasma. Nevertheless the calculation predicts correctly both the value of $k_\Theta a_i$ at which the density spectrum maximizes, and the spectral index at high mode numbers /4,6,7,8,9,19/.

2. EXPERIMENTAL RESULTS.

A CO_2 laser forward scattering experiment has been mounted on TEXTOR (Tokamak EXperiment for Technology Oriented Research: R_o = 175 cm, $a \lesssim 50$ cm). The results are described in References /6-9/. Particularly of interest here is that the experiment has demonstrated that

(i) a periodic enhancement of the turbulence level, integrated along a central vertical chord (owing to the small scattering angle), precedes and follows the sawtooth relaxations of the line average density and of the temperature on axis. The maximum enhancement occurs practically simultaneously with the relaxation on the (central) ECE temperature trace. Its rise

time is = 3.6 msec and its decay time is = 10.4 msec; the period of the sawtooth is = 14 msec. The amplitude of the modulation is 60% of the background level. (Fig. 1a); it is worth noting that the observed increase of the turbulence level is maximum when it coincides with the relaxation on axis, which suggests that the apparent irregularity of the scattering signal (Fig. 1a) is due to the imperfect time resolution.

(ii) the turbulence level, integrated along a central vertical chord, is strongly correlated with the density length scale evaluated between the radii r = 20 cm and r = 30 cm: $\langle n^2 \rangle_{k_\theta} \propto L_N^{-5}$ with $L_N = (d\ln N/dr)^{-1}$. This latter conclusion was obtained by monitoring L_N with radio frequency (ICRH) heating. (Fig. 2). A similar correlation is not observed if L_N is evaluated at other radii. Here, as in (i), "turbulence level" refers to the frequency integrated spectrum at a fixed $k_\perp = k_\theta = 24\ cm^{-1}$ ($\Delta k_\theta = 2.3\ cm^{-1}$) (i.e. $k_\theta a_i = 2.34$ for a 20 kG hydrogen plasma at the temperature Te = 0.4 keV prevailing at the radius r = 25 cm). θ is the poloidal angle.

(iii) the increase within the frequency spectrum (for $k_\theta = 24\ cm^{-1}$) triggered by the sawtooth relaxations occurs mainly in the low frequency range. Fig. (3) shows that the dominant spectral component (f_o = 140 khz) is particularly enhanced which leads to a narrowing of the spectrum at the peak of the sawtooth ($f/\Delta f \simeq 2$, Δf being limited by the finite bandwidth of the filters)

These observations, to our knowledge obtained on a tokamak for the first time, imply that a small perturbation of the line average density ($\lesssim 2\%$) and of the temperature ($\sim 12\%$) are sufficient to induce a finite modification of the turbulence level ($\sim 60\%$). Likewise, a small change in the density length scale (e.g.20%), and presumably in the temperature length scale (not recorded continuously), correlates to a finite (x2.25) modification of $\langle n^2 \rangle_{k_\theta}$. The turbulence level is thus shown experimentally to be a very sensitive function of the local plasma parameters suggesting that indeed $\langle n^2 \rangle$, and by extension K_e, are actually sensitive functions of the linear growth rate γ_L of the instability driving the turbulence.

By starting 3.6 msec before the relaxation of the central electron temperature, the enhancement of the turbulence level shows that energy is already leaking out of the core before the expanding magnetic island - which, according to Kadomtsev /20/ and others /21,22/, triggers this relaxation - has reached the magnetic axis; this time delay is believed to provide valuable information on the expansion velocity of the island.

3. THEORETICAL MODEL.

Our purpose here is to show that the modulation of the turbulence level can be reproduced quantitatively with the help of a numerical code in which the anomalous electron heat transport coefficient is fitted to a set of values calculated consistently from the theoretical fluctuation spectra provided by the saturation theory of the dissipative trapped electron instability described in References /13,14/ (no fitting parameter!).

The ion conduction coefficient is taken to be three times the neoclassical value of Hinton and Hazeltine /23/ but the results of the code are essentially independent of the ion neoclassical anomaly. The theoretical anomalous electron heat conduction coefficient is thus, with the notations of Reference /14/:

$$K_{e,th} = \frac{5<\alpha>_\theta}{3}\left(\frac{m_e}{m_i}\right)^{1/2}\frac{\tau^{1/2}}{k_{rc}^5\, a_i^5}\,\nu^{*-1}\, b_p(\nu^{*1/2})\, G_1\,\frac{a_s^2\, c_s}{|L_s|}$$

$$= \frac{0.71}{\sqrt{A_i}}\,\nu^{*-1}\, b_p(\nu^{*1/2})\, G_1\,\frac{a_s^2\, c_s}{|L_s|} \qquad (1)$$

where $G_1(r)$ is an integral over all wave lengths and frequencies of the fluctuation spectrum. It can be approxima-

ted by $G_1(r) = (1+0.6d_p)\ \bar{G}_1(r)$; $G_1(r) = g(E)h(c)$; c is the parameter defined in Eq. (14-7b) (equation 7b of Reference 14), and $E = L_N / qR\hat{\sigma}$. The other definitions are

$$h(c) = (c-2)^{4.63} \tag{2a}$$

$$g(E) = a_1[1-\exp(-a_2 x)]\ \frac{1+a_3 x}{1+a_4 x + a_5 x^2} \tag{2b}$$

with the numerical coefficients $a_1 = 8120$, $a_2 = 7.87$, $a_3 = 1.54$, $a_4 = 3.685$, $a_5 = 0.0707$, and $x = E - E_0$. The function g(E) and the instability threshold $E_0 = 0.004$ E [alternatively the function h(c)] was obtained by fitting the exact results (calculated from the theoretical spectrum) for c = 10 (for E = 0.09); c = 2 is the absolute instability threshold. We note that c(r) and E(r) are the only two independent parameters entering the normalized growth rate $\tilde{\gamma}_L(r)$ (Eq. 14-7a) which itself determines completely the spectrum (Eq. 14-8); rigorously speaking, $G_1(E,c)$ is however no separable function of E and c. Likewise the turbulence level can be fitted by the curve (Eq. 14-21)

$$\frac{|n|^2}{N^2} = \frac{1}{12\pi k_{rc}^4 a_i^4}\ \frac{a_s^2}{|L_N L_s|}\int_0^\infty dy\ y^{-3/2}\ \bar{f}$$

$$= 0.54\ \frac{a_s^2}{|L_N L_s|}\ g^*(E)\ h^*(c) \tag{3}$$

where $g^*(E)$ has the form (2b) with $a_1^* = 5.60\times10^{-2}$, $a_2^* = 26.17$, $a_3^* = 3.54$, $a_4^* = 3.16$, $a_5^* = 0$; $g^*(E_0) = 0$; furthermore $h^*(c) = (c-2)^{2.22}$.

At present, we have not attempted to solve consistently the

continuity equation in order to avoid the arbitrariness connected with particle transport: indeed, a phenomenological pinching effect is still requested in order to explain the observed density profiles /24/.The density profile is thus frozen to a suitable time average provided by the experiment. This procedure, however, leads to a systematic underestimate of the period of the sawteeth. To remedy this situation, we have assumed the amplitude of the density relaxation $\Delta N/N = \alpha \Delta T_e/T_e$; experimentally $\alpha \leq 2/3$ in TEXTOR; for the shot considered here, $\alpha = 0.5$.

Since the trapped electron mode is stable in the neighbourhood of the magnetic axis, the electron conduction coefficient (1) leads to a peaking of the central temperature - at least if the ion neoclassical transport is small, which is the case at low densities-. The central value of the safety factor has thus a tendency to drop below unity, which, naturally, leads to the onset of the tearing instability; the latter develops into a magnetic island which triggers the sawtooth relaxation. As suggested by the experimental results, we have assumed that the magnetic island invades the core progressively. More specifically, after the safety factor on axis has reached a value $q_{0,c}$, we switch on large electron and ion heat transport coefficients $K_{e,\infty}$ and $K_{i,\infty}$ in the flux tube limited by the magnetic surfaces $r_0(t)$ and $r_2(t)$ of equations

$$r_0(t) = r_1(t)(1 - t/\tau) \qquad (4a)$$

$$r_2(t) = r_1(t)[1 + (\sqrt{2} - 1)\, t/\tau] \qquad (4b)$$

where $r_1(t)$ is the radius of the q=1 surface. (t = 0 is the switch-on time). We note that $(r_2 - r_0)/(r_1 - r_0) = \sqrt{2}$. At time $t = \tau$, $r_0 = 0$; we then switch off the large transport coefficients K_∞; the safety factor on axis recovers thereafter.

The time scale τ should be related to the growth rate of the tearing instability (see /25/,/21/, and References herein):

$$\gamma_T^* = \frac{\gamma_T^3}{|\omega_e^* \omega_i^*| (1+1.71\eta_e)(1+\eta_i)} \qquad (5)$$

where $\gamma_T = \tau_R^{-1/3}\tau_H^{-2/3}$ is the Furth-Killeen-Rosenbluth growth rate /26/ for negligible density gradients ($\omega^* \ll \gamma_T$); $\tau_R = 2\pi r_1^2 \sigma_{\parallel}/c^2$ (respectively $\tau_H = L_S/C_A$) is the resistive (the hydromagnetic) time scale; $\sigma_{\parallel}$ is the parallel Spitzer conductivity and C_A the Alfvèn velocity. The transprot coefficients $K_{e,\infty}$ and $K_{i,\infty}$ are related to the free streaming (except for the build up of an ambipolar potential) along perturbed magnetic field lines having a radial component, and therefore to the saturation level of the tearing instability.

Present theories do not provide the relation linking τ and K_∞ on the one hand and γ_T^* on the other hand. We shall assume $\gamma_T^* \tau \sim 5$ and $K_{e,\infty} = K_{i,\infty} = 2 \times 10^5 cm^2 sec^{-1}$. The justification for retaining here ion transport is that experiment has shown that the sawteeth have a cleaning action on the impurities. We note that the results we obtain are largely independent of these choices; however when K_∞ is increased above a certain value, the peak of the turbulent signal in Fig. 1b becomes larger and narrower.

Neither the sawtooth model of Kadomtsev /20/ nor that of Dubois and Samain /22/ specify the critical safety factor $q_{o,c}$ for which the relaxation occurs (alternatively the radius of the corresponding q = 1 surface) although we note the attempt by Parail and Pereverzev /27/ to resolve this question. As in other works /28,29/, $q_{o,c}$ is thus chosen to yield the correct relative amplitude of the electron temperature relaxation on axis.

In view of the inadequacies (which have still been exemplified by the recent experimental results of Soltwisch et al /30/) of the existing relaxation models, we have chosen to simplify the calculation by assuming that the current density J is proportional to $Te^{3/2}$ (Spitzer conductivity). This implies that we

assume instantaneous penetration of the magnetic field (no skin effect). This hypothesis has as a consequence that the calculated sawtooth period is too short, but has virtually no impact on what is here our main concern, i.e. the calculation of the enhancement of the turbulence signal outside the core by the internal relaxations. (We note however that when the skin effect is taken into account, we observe the formation of hollow current profiles in agreement with the discussion developed in Ref. /27/.)

The trapped electron instability is inadequate to assume the transport in the cold outer plasma layers characterized by a high collisionality parameter ν^* (defined in /14/). We limit therefore our numerical calculations to the region $r \lesssim 40$ cm. The boundary electron temperature is taken over from experiment (it is determined by Thompson scattering 100 msec later), but we note that the results from the code are not affected by moderate changes in T_b. In view of the small equipartition time at the plasma boundary, we assume $T_{i,b} = T_{e,b}$. We also remark that the numerical code forces the temperature modulation, due to the heat pulse, to vanish at the boundary.

4. NUMERICAL RESULTS.

Assuming $K_{e,\infty} = K_{i,\infty} = 2 \times 10^5$ cm^2 sec^{-1} and $\tau = 2.5$ msec (i.e. $\vartheta_T^* = 5.7$ if $\hat{\sigma} = 0.1$ and $L_N = 50$ cm), the constraint set on the amplitude of the temperature relaxation on axis is satisfied when $q_{o,c} = 0.888$ for the discharge considered (TEXTOR shot 11183, 0.8 sec $\lesssim t \lesssim$ 0.9 sec, $I_p = 339$ kA, $B_t(0) = 2.02$T, $\langle N \rangle = 2.2\ 10^{13}$ cm^{-3}, $Z_{eff} = 1.6$, $\Delta T_o/T_o = 11.5\%$; $\langle N \rangle$ being the volume average density).

4.1 Global Plasma Parameters

The inner transport coefficients K_∞ are introduced when $q_0 = q_{0,c} = 0.888$, and, consistently $r_1 = (r_1(t))^{Max} = 16.2$ cm; the safety factor on axis continues to fall thereafter until the magnetic island reaches the center of the discharge at which time $q_0 = q_0^{min} = 0.839$. Meanwhile the temperature profiles have the form shown in Fig. 4a where one sees clearly the effect of the island. (time $t = \tau/2$ after the introduction of K_∞). The central cone appearing in Fig. 4a shrinks later on and completely disappears for $t = \tau$, at which time the safety factor on axis very suddenly jumps to $q_0 = q_0^{Max} = 0.994$. The inner transport coefficient is then removed. Subsequent heating associated to a good thermal insulation of the core lowers q_0 until it reaches the value $q_{0,c}$ when the whole process is repeated. The temperature profile is shown in Fig. 4b at the time of switch on and of switch off of K_∞. It is seen that it does not practically change outside the q=1 surface (r = 16.2 cm). Our model thus explains the "profile consistency" reported by Coppi /31/ and clearly observed in JET discharges /32/. The calculated central temperature 771 eV $\leqslant T_{e,o} \leqslant$ 865 eV, loop voltage 1.15 V $\leqslant U \leqslant$ 1.17 V, energy confinement time τ_E = 53 msec., and sawtooth period $\tilde{\tilde{\tau}}$ = 9.24 ms, are in satisfactory agreement with the measured values $T_{e,o}$ = 687 eV (as determined by Thompson scattering 100 ms after the laser scattering experiment), U = 1.31 V, τ_E = 27 msec (obtained by diamagnetic loops), and $\hat{\tilde{\tau}}$ = 14 msec. As concerns the energy confinement time, the difference between the calculated and the measured values is clearly within the possible errors introduced by the radiation losses (not included in the code). As regards the period, we note that the measured values of $T_{e,o}$, $\Delta T_{e,o}$, N_o ($=3.12\times10^{13}$cm^{-3}), U, Z_{eff}, and $\tilde{\tilde{\tau}}$ are inconsistent, leading to $\tilde{\tilde{\tau}} = 3(1+\alpha)\, N_o \Delta T_{e,o}/\sigma_{\parallel,o}\, E^2 = 6.33$ msec. The paradox can be removed satisfactorily only if we note that the loop voltage is measured at the periphery, and that the value on axis can be appreciably lower in view of the long current penetration time. (The numerical calculation including the skin effect has shown that $V_{axis}/V_{boundary} = 0.69$).

4.2 Microturbulence and Local Plasma Properties.

Fig 1b shows the turbulence spectrum integrated over frequencies and mode numbers, and averaged over the plasma radius. This calculated signal has obviously the same form as the measured one (Fig. 1a) although the latter corresponds to the frequency - integrated spectrum at $k_\theta = 24\ cm^{-1}$. Particularly striking is the amplitude of the modulation (respectively 66 % and 62 %). The relative fluctuation level $\sqrt{\langle n^2 \rangle}/N$ is obtained by dividing the numerical values shown in Fig. 1b by a local density in the scattering volume; we thus obtain

$$\left(\frac{\sqrt{\langle n^2 \rangle}}{N}\right)_{th} \sim 3.2 \times 10^{-3}$$

Extrapolation of the turbulence level measured in a limited region of k_θ- space has led, for similar plasma parameters to the estimate $(\sqrt{\langle n^2 \rangle}/N)_{exp} \simeq 4 \times 10^{-3}$ (window t_2 in the table p.56 and in Fig. 4.1 of Reference /7/)

The code shows that the turbulence level reaches its largest value at the radius r = 27 cm (see Fig. 5) during most of the sawtooth period; this radius however decreases to r = 20 cm during the first couple of milliseconds following the introduction of the magnetic island. Fig. 5 also shows that $\langle n^2 \rangle$ has decreased by a factor of 2 at the radii r = 19 cm and r = 36 cm. These theoretical results agree with the observation that the central line-integrated turbulence level correlates well with the density length scale evaluated between 20 and 30 cm but does not correlate with the value of L_N evaluated at other plasma radii.

Another prediction of the code is the periodic enhancement of the electron heat transport coefficient K_e by a factor 4.15 at the radius r = 25 cm and 2.3 at r = 40 cm (Fig. 6). The electron heat flux $r\phi_e = rK_eN\,\partial T_e/\partial r$ is modulated similarily (Fig. 7). These examples show that, in our model, energy is

released in bursts in contrast to the laminar transport picture of Kadomtsev and Pogutse /10/, Horton and Estes /11/, Molvig, Hirshman and Whiston /12/, and others. We note that the existence of an enhanced heat flux on the limiter after each internal disruption has been clearly seen on other machines, e.g. TFR 600 /17/ and ASDEX /18/. We quote (/17/): "The (internal) disruptions seem to affect the energy transport during a relatively large time in a large domain outside the q = 1 surface. Indeed, while no significant variation of the magnetic activity detected at the plasma edge is observed, an energy flux of about 500 kW appears at the limiter after each disruption. This fact is hardly understandable without a transient increase by a factor 5-10 of the transport coefficients outside the q = 1 surface. A similar conclusion may be drawn from the observation of bursts of hard X-rays beginning 200 μsec after each disruption."

Yet another output of the code is the evolution of the electron and ion temperatures at different radii (Fig. 8a, b). The average velocity defined by the propagation of the maximum of the electron temperature pulse between the magnetic surface of radius $(r_1(t))^{Max}$ = 16.2 cm and the "boundary" radius r_b = 40 cm is approximately u_p = 1.5 10^4 cm sec^{-1}; a similar result is obtained by considering the curves for the heat flux. The time required by the pulse to reach the physical limiter at r = a = 45.7 cm is approximately 2.0 msec, i.e. more than an order of magnitude shorter than the energy confinement time. Again, similar conclusions have been reached from experimental considerations in other devices, including JET /32/.

Finally, the modifications of the frequency spectrum at fixed k_Θ induced by the relaxation is beyond the scope of our theoretical model for reasons explained in the Introduction.

5. CONCLUSIONS

The CO_2 laser forward scattering experiment installed on TEXTOR /6-9/ has shown that the central line-integrated turbulence level at $k_\perp = k_\theta = 24\ cm^{-1}$ is

(i) modulated by the heat pulses expelled by the sawtooth relaxations, and
(ii) correlated with the density length scale.
(iii) The experiment also shows that the frequency spectrum at fixed k_θ gets narrower at the maximum of the sawtooth.

A theory /13,14/ developed by two of the authors provides an anomalous electron heat transport coefficient (no fitting parameter!) which turns out to be a sensitive function of the linear growth rate of the instability. The results of a transport code, developed on this theoretical basis,
(a) are in quantitative agreement with the puzzling observations reported above (no theoretical information can however be drawn concerning the frequency spectrum because of the weak turbulence approach),
(b) predict a modulation of K_e and of the associated heat flux throughout the plasma as suggested by temperature measurements at the limiter /17, 18/ in other devices,
(c) explain the "profile consistency" first suggested by Coppi /31/ and clearly observed in JET discharges /32/, and
(d) yield realistic values for the global plasma parameters (central temperature, loop voltage, confinement time, period of sawteeth).
These results are summarized in Table I.

The picture we have proposed of transport, described in the Introduction, and more specifically the rapid variation of K_e with respect to the linear growth rate (γ_L) of the microinstability, suggests that

(α) scaling laws should not be sought in relation to a local calculation of K_e (as is usually done) since the

latter is a very sensitive function of the chosen plasma parameters;

(β) there is a sharp limit to the performance of each machine owing to the nonlinear relation $K_e(\tau_L)$;

(γ) if this limit is reached in the ohmic regime, then the confinement time will encounter a rapid degradation once auxiliary heating is applied. Preliminary numerical calculation (Fig. 4c) with a peaked auxiliary power deposition profile has verified this intuition: with $P_{Aux} = P_{OH}$, the theoretical confinement time falls from 53 to 34 msec.
The phenomena of degradation and profile consistency are in fact interrelated. The latter is dramatically demonstrated by comparing Fig. 4b and 4c. Experimentally, the degradation of energy confinement is one of the most persistent and worrying features of auxiliary heating /33/ whether by neutral beam injection or by radio frequency waves; it is also a result that no empirical code had been able to foresee;

(δ) similar conclusions should apply, "mutatis mutandis", to pellet fueling experiments. A preleminary run has indeed shown a rapid reshaping of the temperature profile in agreement with the observations on ALCATOR C /34/ and TFR /35/;

(ε) increased shear in the vicinity of the separatrix, leading to an improved stabilization of the trapped electron mode, should allow steeper temperature gradients to develop and probably yield improved confinement in tokamaks with axisymmetric divertors (the so-called H confinement regime /36/).

In view of the encouraging results reported in this paper, we plan to analyse systematically a set of discharges with different magnetic fields, plasma currents, average densities, and auxiliary power levels. We will also extend the code to

follow the evolution of the density profile and the current penetration.

The results described in this paper have been partially reported at the 2nd International Symposium on Laser Aided Plasma Diagnostics, Culham, September 1985, /37/.

Table 1: Summary of results for TEXTOR shot 1183. Input parameters: $B = 20$ kG, $\langle N_e \rangle = 2.2\ 10^{13}$ (volume average), $I_p = 339$ kA, $Z_{eff} = 1.6$, $\Delta T_{e,o}/T_{e,o} = 11{,}5$ %

	Measured	Calculated
Central electron temperature (e.V)	687	$771 \leqslant T_e \leqslant 865$
Loop voltage (V.)	1.31	1.16
Sawteeth period (msec)	14	9.25
Energy confinement time (msec)	27	53
Inversion radius (cm)	$10 < r_1 < 20$	$r_1 = 16.2$
Normalized turbulence level $\sqrt{\langle n^2 \rangle}/N$	4×10^{-3}	3.3×10^{-3}
Modulation of the turbulence level	62 %	66 %
Modulation of the heat flux at 25 cm		430 %
Modulation of the heat flux at 40 cm		260 %
Average propagation velocity of the heat pulse (cm sec^{-1})		1.5×10^4
Radius of maximum turbulence level (cm)	$20 < r < 30$	$r = 27$

REFERENCES

1. Slusher, R.E., Surko, C.M., Phys. Fluids 23 (1980) 473; Watterson, R.L., Slusher, R.E., Surko, C.M. Phys. Fluids (1985) 2857.
2. Mazzucato, E., Phys. Rev.Lett. 48 (1982) 1828
3. Evans, D.E., Doyle, E. J., Frigione, D., von Hellermann,M., Murdoch, A., Plasma Phys. 25 (1983) 617
4. TFR Group and Truc,A., Plasma Phys. and Controlled Fus., 26 (1984) 1045
5. Brower, D.L., Peebles, W.A., Luhman, N.C., Savage, R.L., Jr., Phys.Rev.Lett. 54 (1985) 689
6. Boileau, A., Thèse de Maitrise, Université de Montreal (1985): "Mesure des Fluctuations de Densité Electronique dans les Plasmas à l'Aide de la Diffusion d'un Faisceau Laser CO_2"
7. Van Andel, H.W.H., MAS Report 24 SU, 31926-3-0017, Div. of. Energy, Nat. Res. Council, Ottawa, Canada (1985) "Plasma Fluctuation Measurements on TEXTOR Using CW CO_2 Laser Scattering".
8. Von Hellermann, M., Univ. of Essen Report (1985) "Fluctuation Measurements on the TEXTOR Tokamak by Forward Scattering in the Infrared"
9. Van Andel, H.W.H., Boileau, A., von Hellermann, M., Proc. 2nd International Symposium on Laser Aided Plasma Diagnostics, Culham (1985).
10. Kadomtsev, B.B., Pogutse, O.P., in Plasma Physics and Controlled Nuclear Fusion Research 1978, Vol 1., IAEA, Vienna (1979) 649
11. Horton, W., Jr., Estes, R.D., Nucl. Fus. 19 (1979) 203.
12. Molvig, K., Hirshman, S.P., Whiston, J.C., Phys.Rev.Lett. 43 (1979) 582
13. Rogister, A., Hasselberg, G., Phys.Rev.Lett. 48 (1982) 249, and Phys. Fluids 26 (1983) 1467
14. Hasselberg, G., Rogister, A., Nucl. Fus. 23 (1983) 1351
15. Rogister, A., Hasselberg, G., Kaleck, A., Waelbroeck, F., in Plasma Physics and Controlled Nuclear Fusion Research 1984, Vol.2, IAEA, Vienna (1985) 139
16. Paul, J.M.W., Daughney, C.C., Holmes, L.S., Nature 223 (1969) 822

17. TFR Group, in Heating in Toroidal Plasmas 1980, Vol 2, CEC, Brussels and Luxembourg (1981) 723
18. Bein, B.K., Müller, E.R., Journal Nucl. Mat. 111 and 112 (1982) 548; Müller, E.R., Bein, B.K., Steinmetz, K., Max Planck Institut Report IPP III/97 (1984):"Time and Space-Resolved Energy Flux Measurments in the Divertor of the ASDEX Tokamak by Computerized Infrared Thermography"
19. Semet, A., Hase, A., Peebles, W.A., Luhman, N.C., Jr., Zweben, S., Phys.Rev.Lett. 45 (1980) 445
20. Kadomtsev, B.B., Fiz. Plasmy 1 (1975) 710 (Sov. J. Plasma Phys.)
21. Jahns, G.L., Soler, M., Waddell, B.V., Callen, J.D., Hicks, H.R., Nucl. Fus. 18 (1978) 609
22. Dubois,M., Samain, A., Nucl. Fus. 20 (1980) 1101
23. Hinton, F.L., Hazeltine, R.D., Rev. Mod. Phys. 48 (1976) 239
24. Coppi, B., Sharky, N., Nucl. Fus. 21 (1981) 1363
25. Rogister, A., Hasselberg, G., in Plasma Physics and Controlled Nuclear Fusion Research 1978, Vol. 1, IAEA, Vienna (1979) 809.
26. Furth, H.P., Killeen, J., Rosenbluth, M.N., Phys. Fluids 6 (1963) 459.
27. Parail, V.V., Pereverzev, G.V., Fiz. Plasmy 6 (1980) 27 Sov.J. Plasma Phys. 6 (1980) 14 .
28. Dnestrovskii, Yu.N., Lysenko, S.E., Smith, R., Fiz. Plasmy 3 (1977) 18 Sov.J. Plasma Phys. 3 (1977) 9.
29. Capes, H., Mercier, C., Morera, J.P., Quang H.A., Cissoko, G., in Heating in Toroidal Plasmas 1984, Vol. 2., Monotypia Franchi, Città di Castello (Perugia), Italy (1984) 921.
30. Soltwisch, H., Stodiek, W., Kaleck, A., Schlüter, J., Current Distribution and Magnetohydrodynamic Activity in TEXTOR Tokamak, Bull. Am. Phys. Soc. 30 (1985) to appear.
31. Coppi, B., in Physics of Plasmas Close to Thermonuclear Conditions, Varenna (1979), Vol. II, 479.
32. Rebut, P.H., Brusati, M., in Controlled Fusion and Plasma Physics 1985, Budapest (1985) to appear.
33. Goldston, R.J., in Controlled Fusion and Plasma Physics 1983, Plasma Phys. 26 (1984) 87.

34. Greenwald, M., Gwinn, D., Milora, S., Parker, J., Wolfe, S., Besen, M., Blackwell, B., Camacho, F., Fairfax, S., Fiore, C., Foord, M., Gandy, R., Gomez, C., Granetz, R., LaBombard, B., Lipschultz, B., Lloyd, B., Marmar, E., McCool, S., Pappas, D., Petrasso, R., Porkolab, M., Pribyl, P., Rice, J., Schuresko, D., Takase, Y., Terry, J., Watterson, R., in Plasma Physics and Controlled Nuclear Fusion Research 1984, Vol. 1, IAEA, Vienna (1985) 45.
35. Equipe TFR, in Plasma Physics and Controlled Fusion Research 1984, Vol. 1, IAEA, Vienna (1985) 103.
36. Wagner, F., Becker, G., Behringer, K., Campbell, D., Eberhagen, A., Engelhardt, W., Fussmann, G., Gehre, O., Gernhardt, J., v. Gierke, G., Haas, G., Huang, M., Karger, F., Keilhacker, M., Klüber, O., Kornherr, M., Lackner, K., Lisitano, G., Lister, G.G., Mayer, H.M., Meisel, D., Müller, E.R., Murmann, H., Niedermeyer, H., Poschenrieder, W., Rapp, H., Röhr, H., Schneider, F., Siller, G., Speth, E., Stäbler, A., Steuer, K.H., Venus, G., Vollmer, O., Yü, Z., Phys. Rev. Lett. 49 (1982) 1408.
37. Rogister, A., Hasselberg, G., Kaleck, A., Boileau, A., Van Andel, H.W.H., von Hellermann, M., Proc. 2nd International Symposium on Laser Aided Plasma Diagnostics, Culham (1985) 7.

FIGURE CAPTIONS.

1. Line average turbulence level obtained (a) experimentally at $k_\Theta = 24\ cm^{-1}$ ($\Delta k_\Theta = 2.3\ cm^{-1}$); (b) theoretically after integration over $\vec{k}_\perp$
2. Correlation between the central line-integrated turbulence level and the density length scale evaluated between the radii r = 20 cm and r = 30 cm (experimental result, log-log scale). The index "0" refers to the ohmic plasma.
3. Density fluctuation frequency spectrum at the maximum and at the minimum of the sawtooth ($k_\Theta = 24\ cm^{-1}$, $k_\Theta = 2.3\ cm^{-1}$).

4. a) Electron and ion temperature profiles obtained numerically at t = 1.25 msec after the birth of the expanding magnetic island; b) Electron temperature profiles at the switch on (continuous line) and switch off (dashed lined) times of the island; c) Same as in (b) for a similar discharge with auxilliary heating ($P_{Aux} = P_{OH}$).
5. Plot of the turbulence level $\langle n^2 \rangle$ as a function of radius (theoretical).
6. Theoretical curves of the anomalous electron heat transport coefficient versus time at the radii (a) r = 25 cm, (b) r = 40 cm.
7. Theoretical curves of the anomalous electron heat flux $r\phi_e = rK_e N \partial T_e/\partial r$ versus time at (a) r = 25 cm, (b) r = 40 cm.
8. Evolution of the electron (a) and ion (b) temperatures at different radii demonstrating the propagation of the heat pulse. (theoretical)

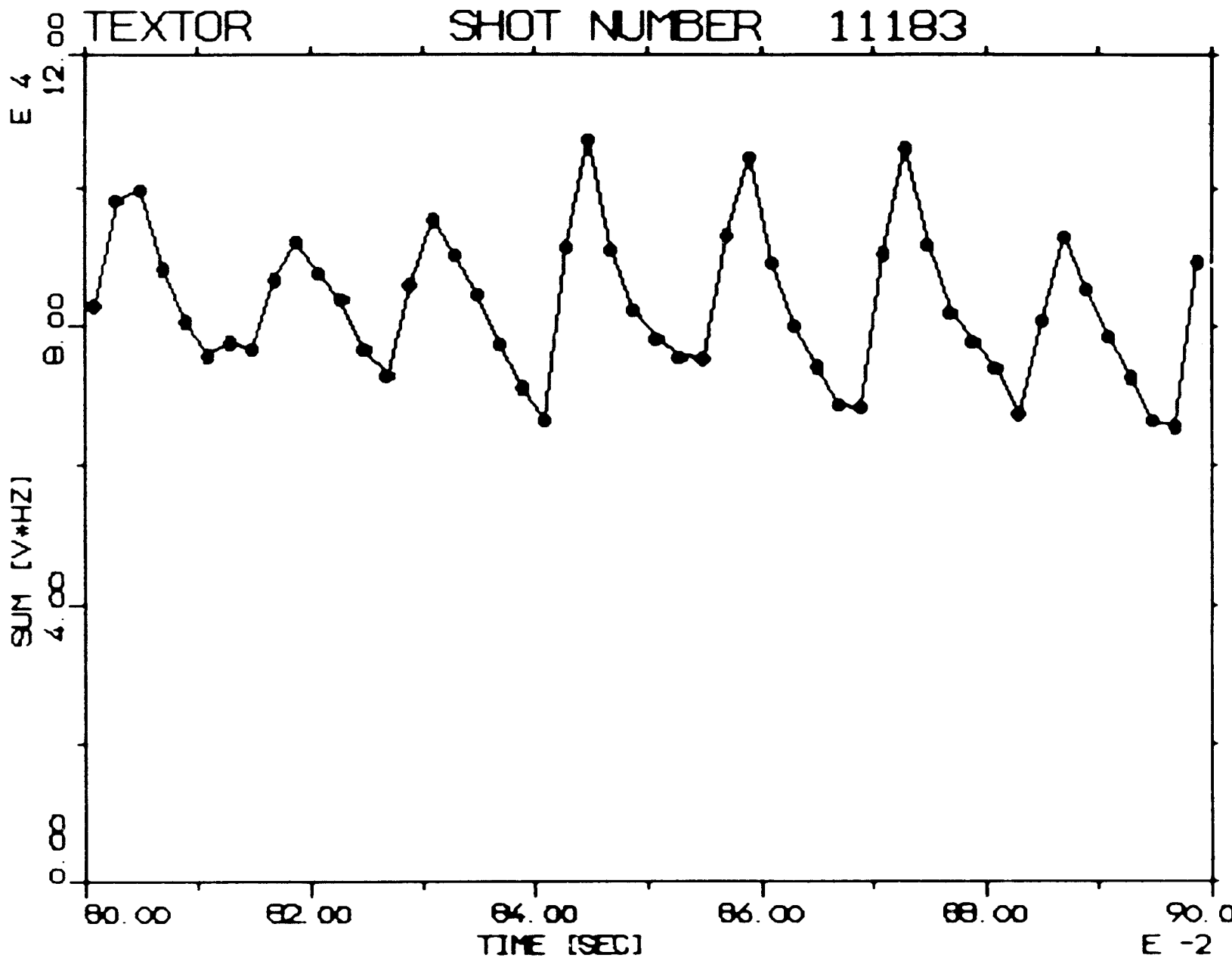
TEXTOR
SHOT NUMBER 11183
E 4
12.00
8.00
4.00
0.00
SUM [V*HZ]
80.00
82.00
84.00
86.00
88.00
90.00
TIME [SEC]
E -2

Fig 1a

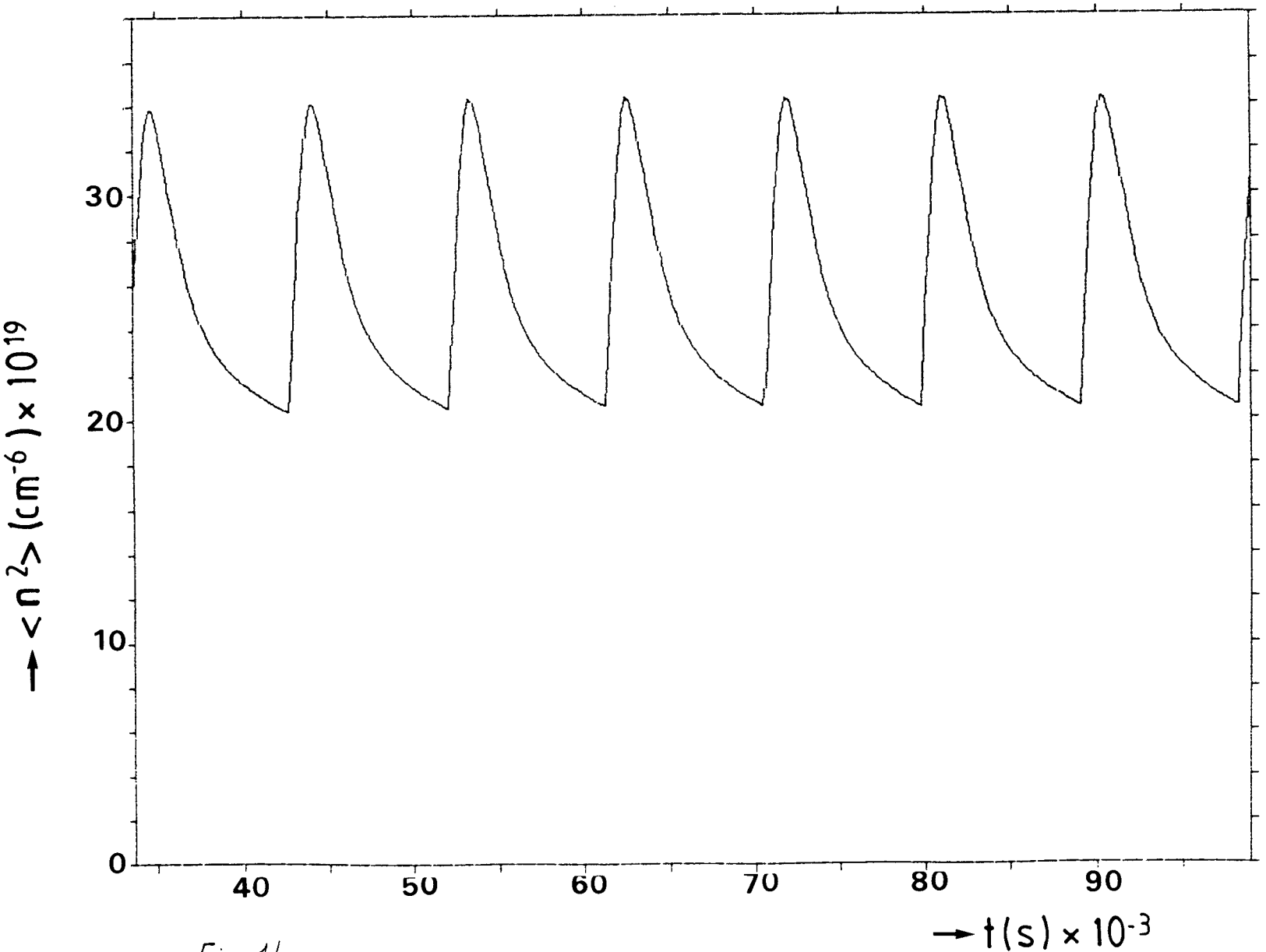

Fig 1b

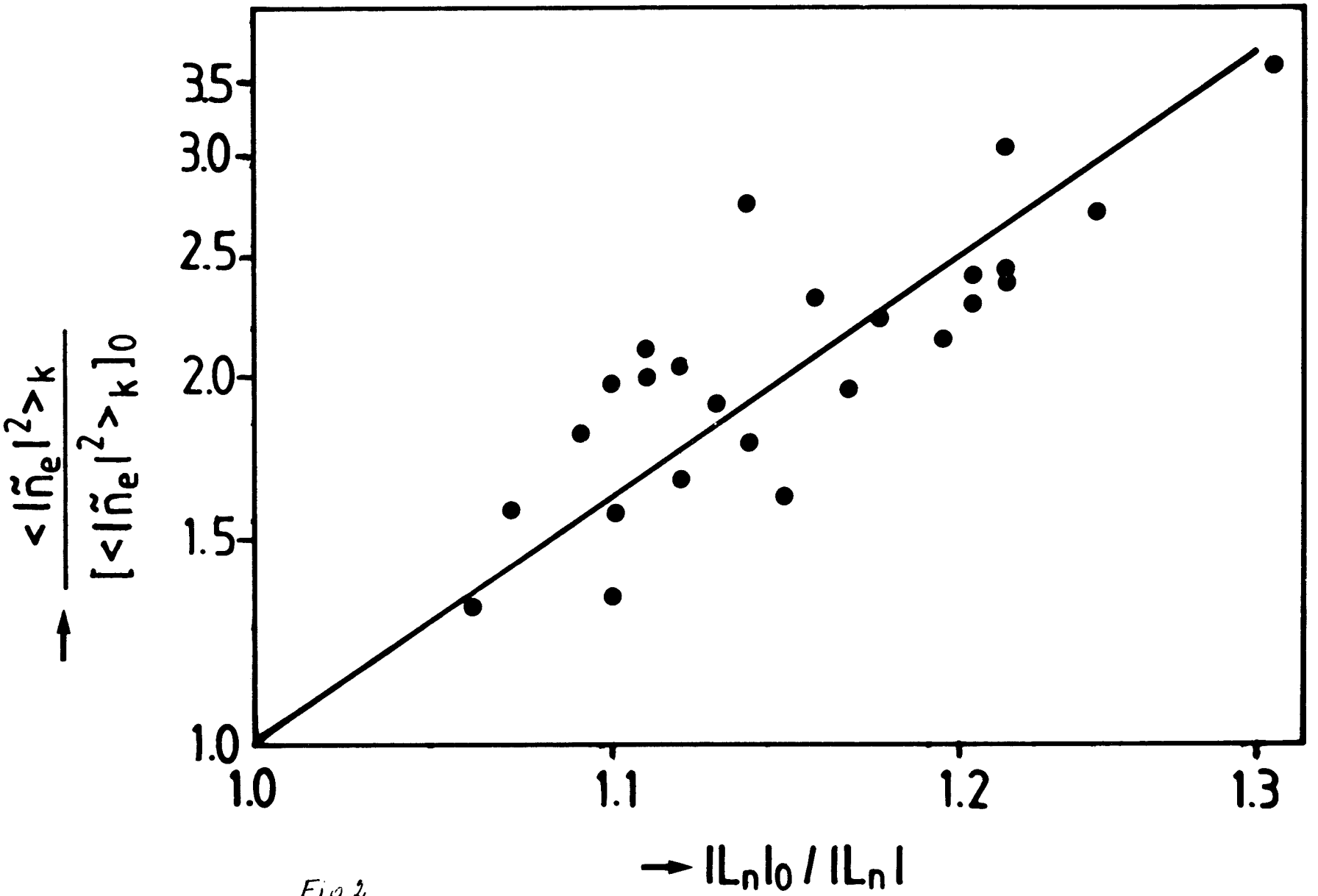

Fig 2

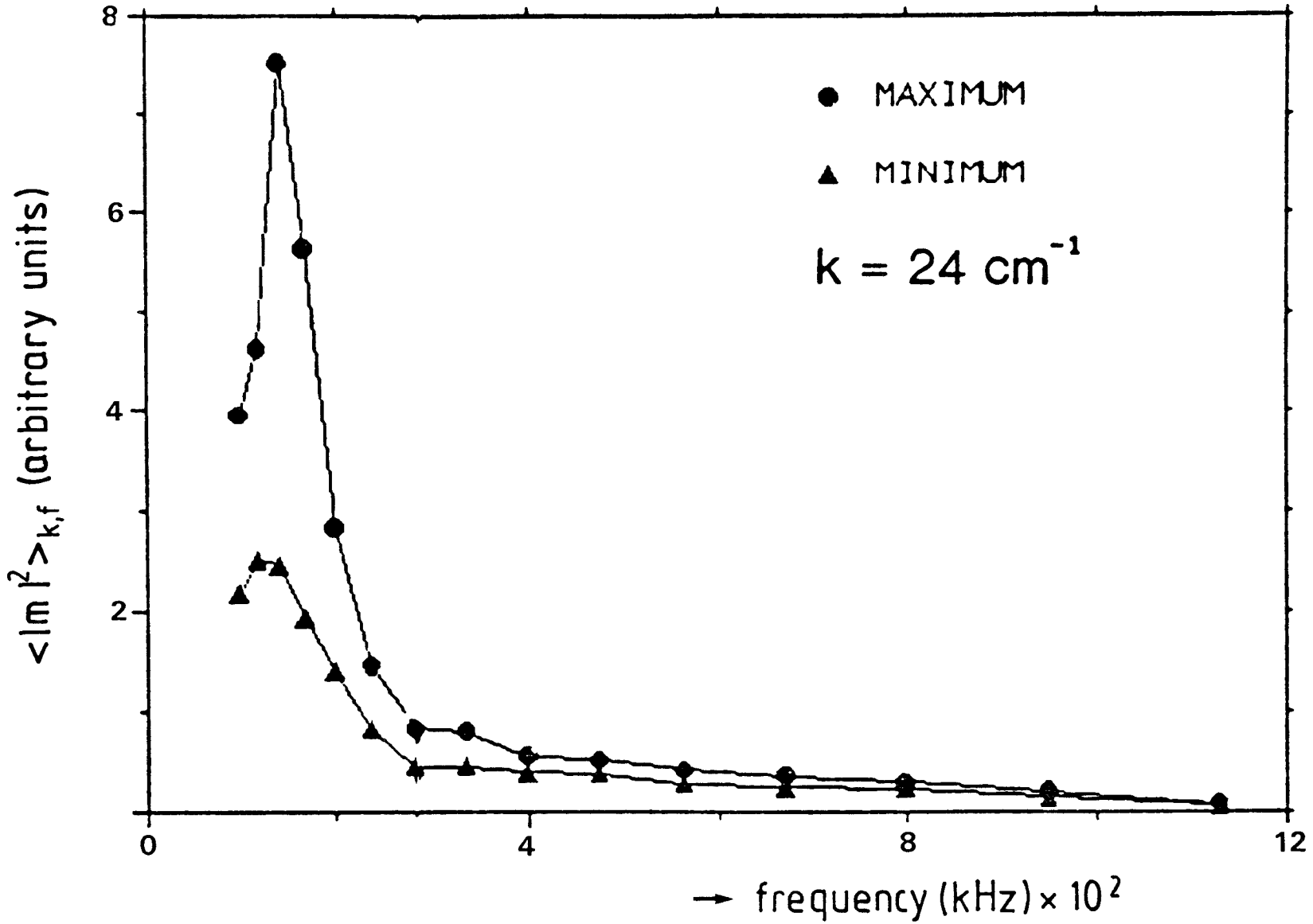
8
6
4
2
0
4
8
12
MAXIMUM
MINIMUM
k = 24 cm^{-1}
$\langle |m|^2 \rangle_{k,f}$ (arbitrary units)
frequency (kHz) × 10^2

Fig. 3

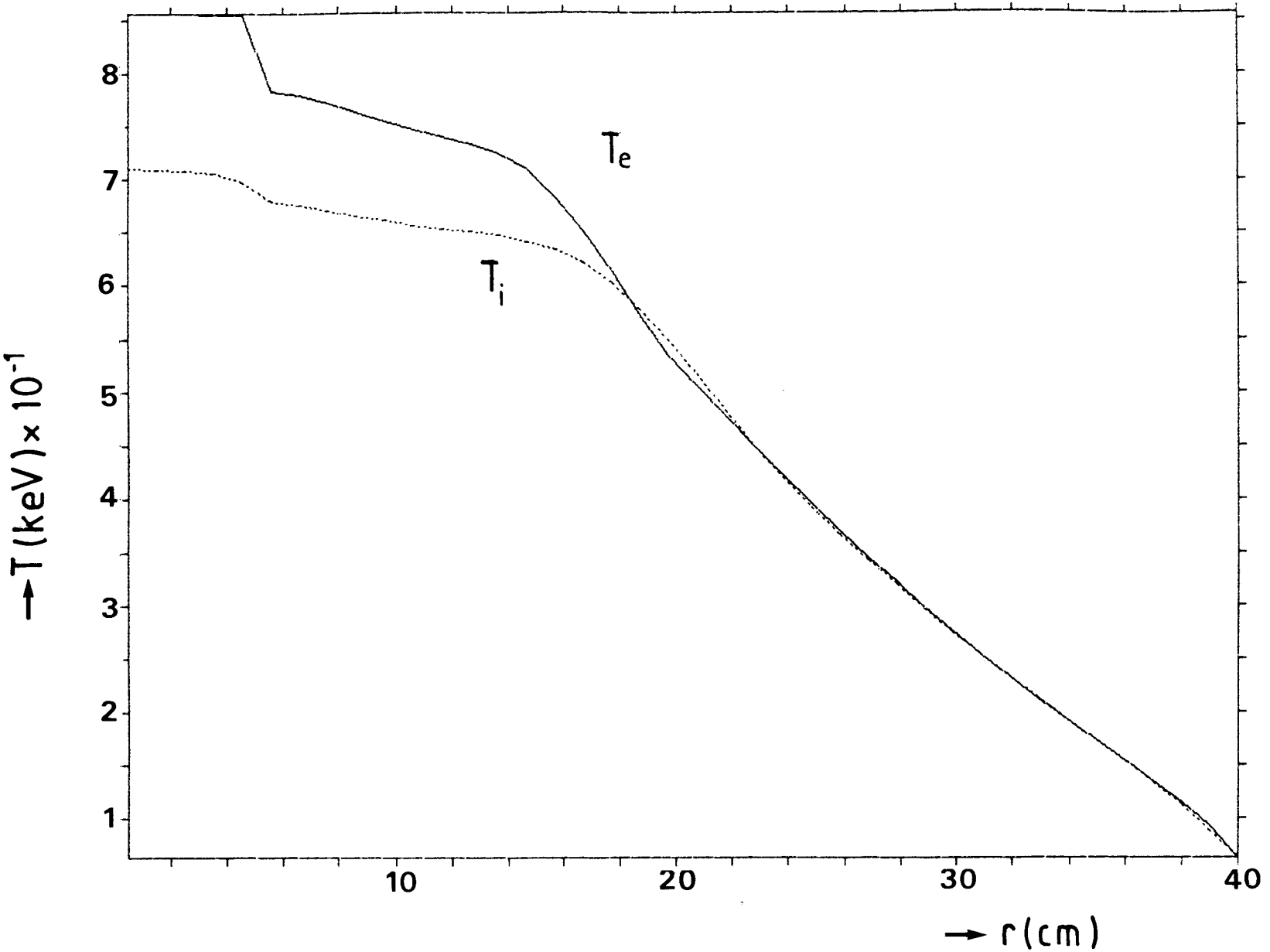

Fig 4a

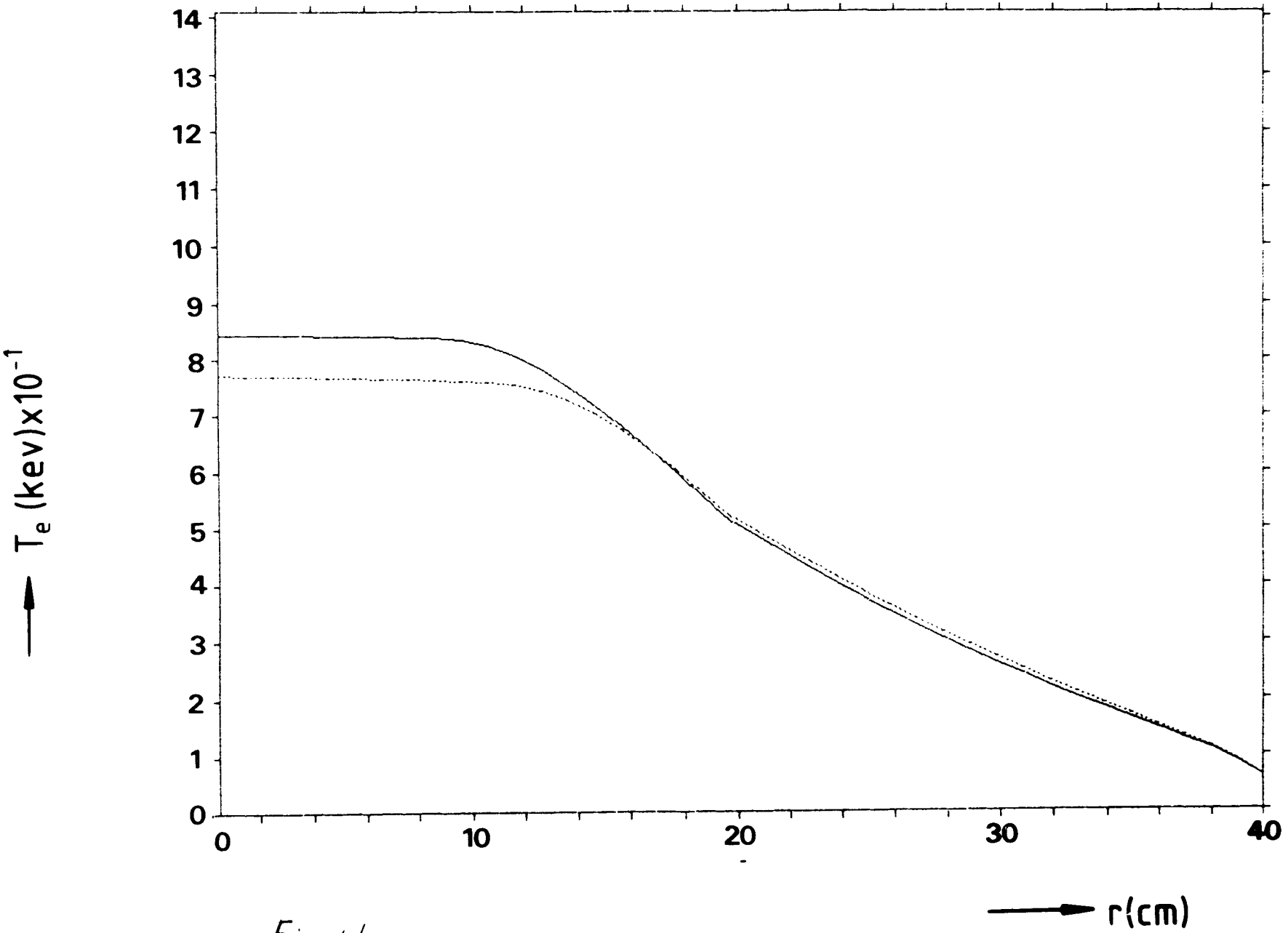

Fig 4b

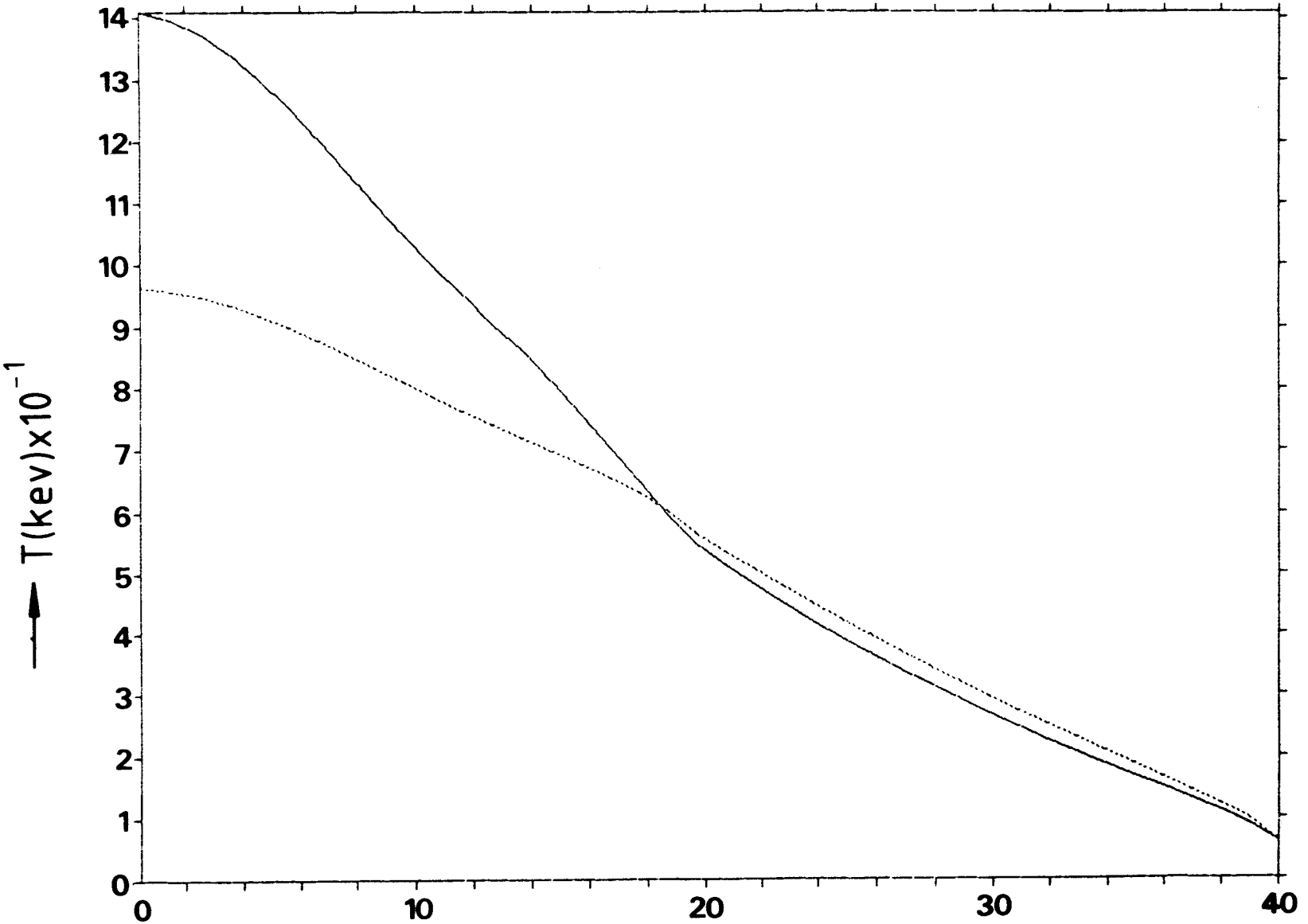

Fig 4c

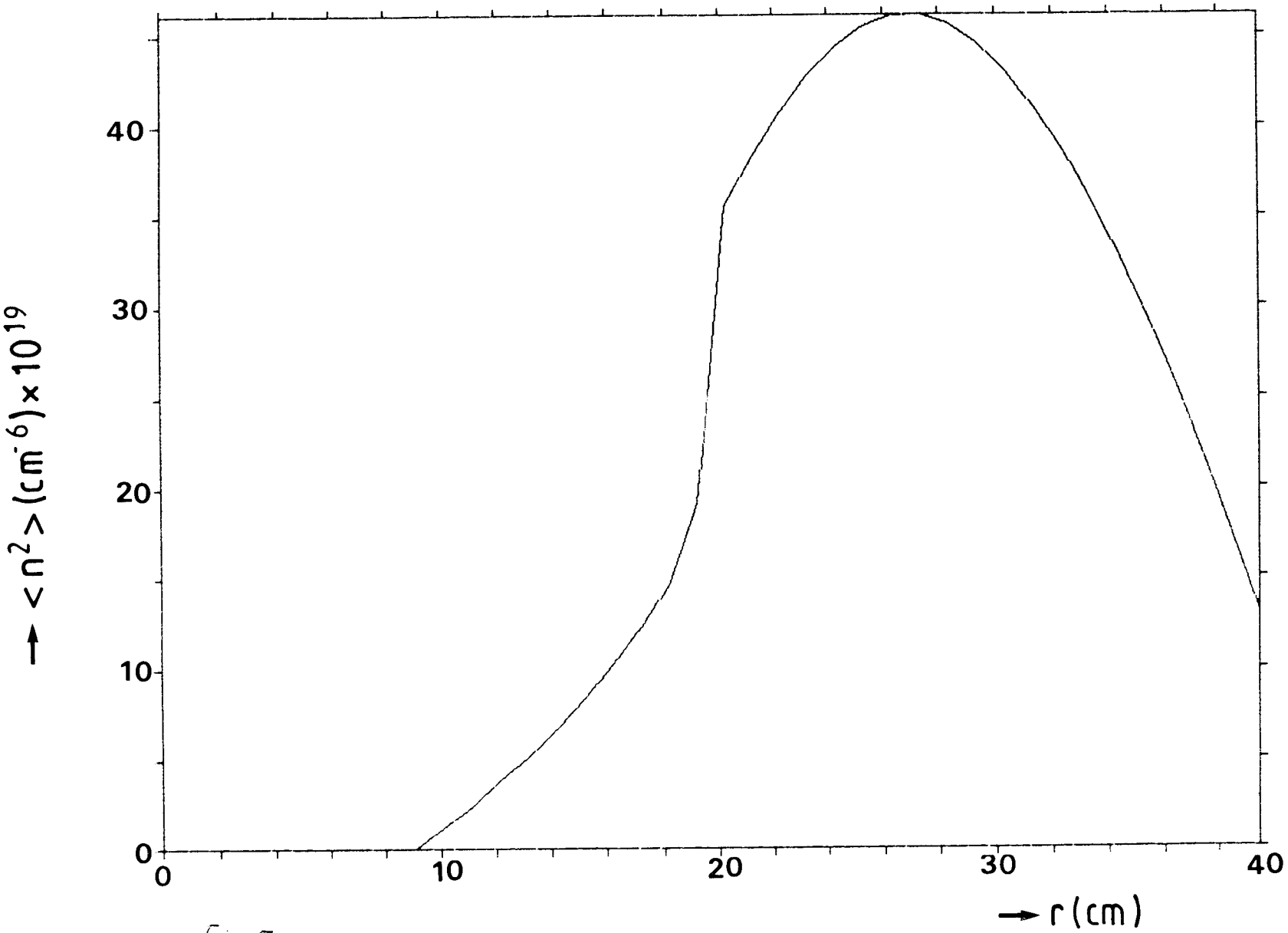
$\rightarrow \langle n^2 \rangle (cm^{-6}) \times 10^{19}$
40
30
20
10
0
0
10
20
30
40
$\rightarrow$ r (cm)

Fig 5

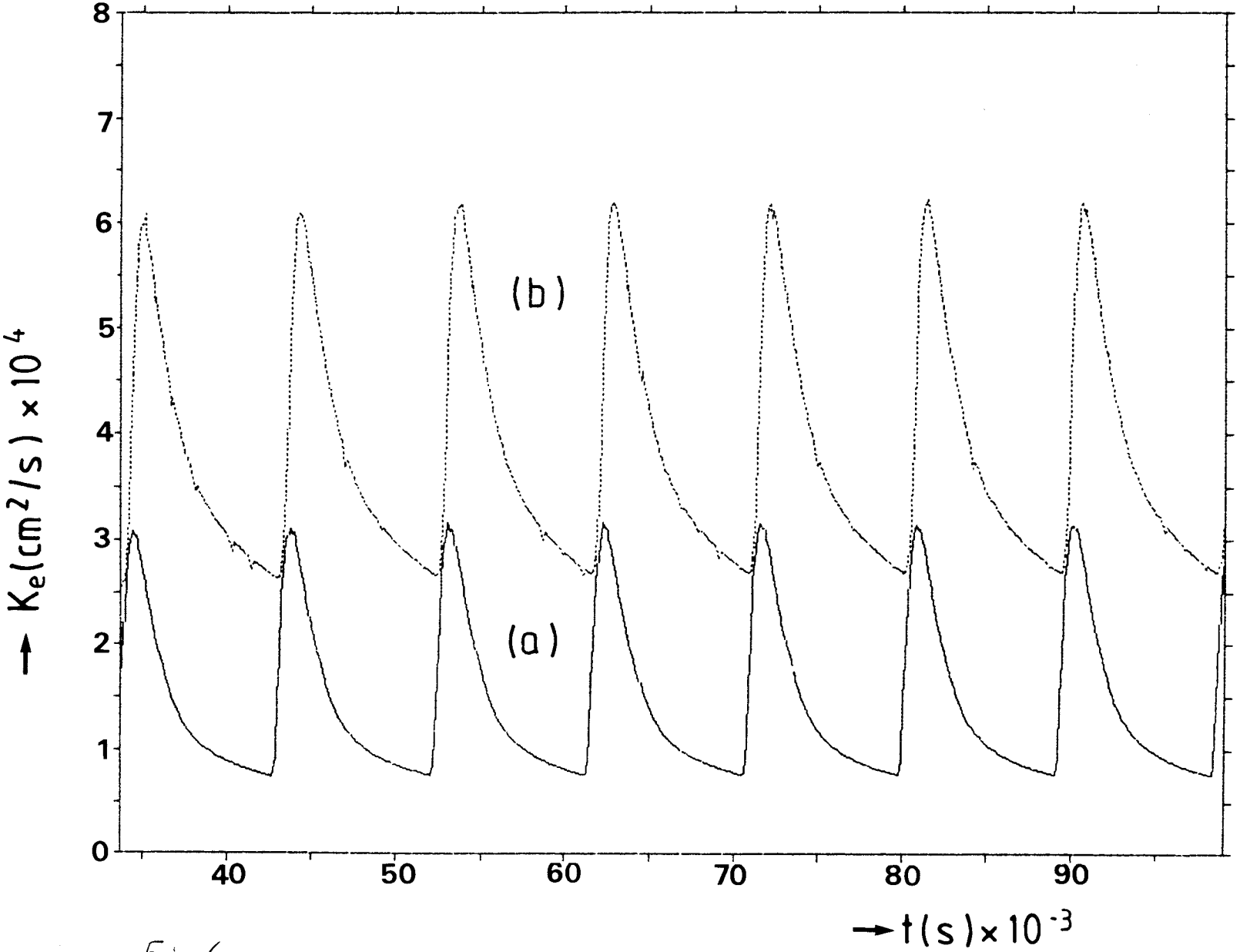

Fig 6

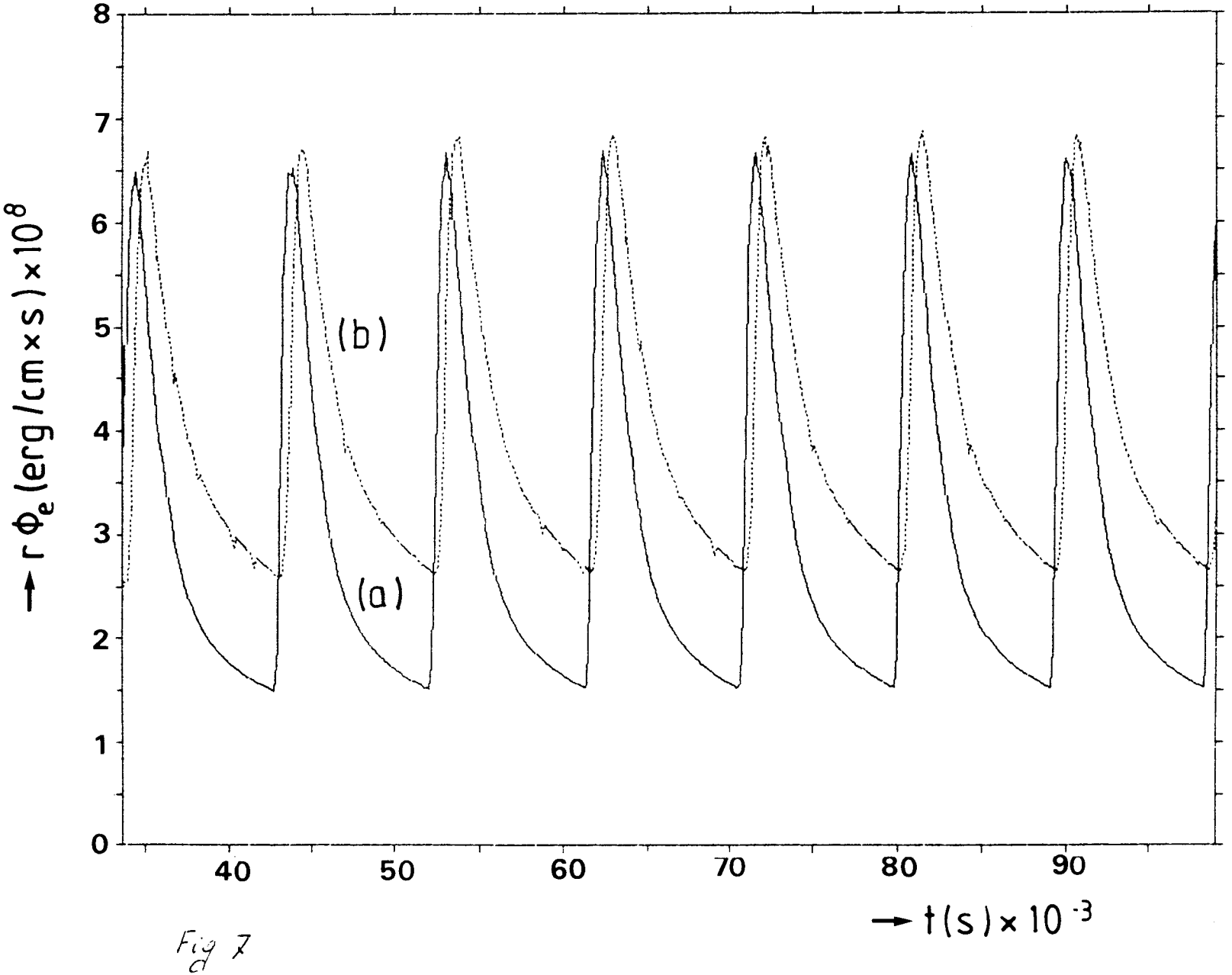

Fig 7

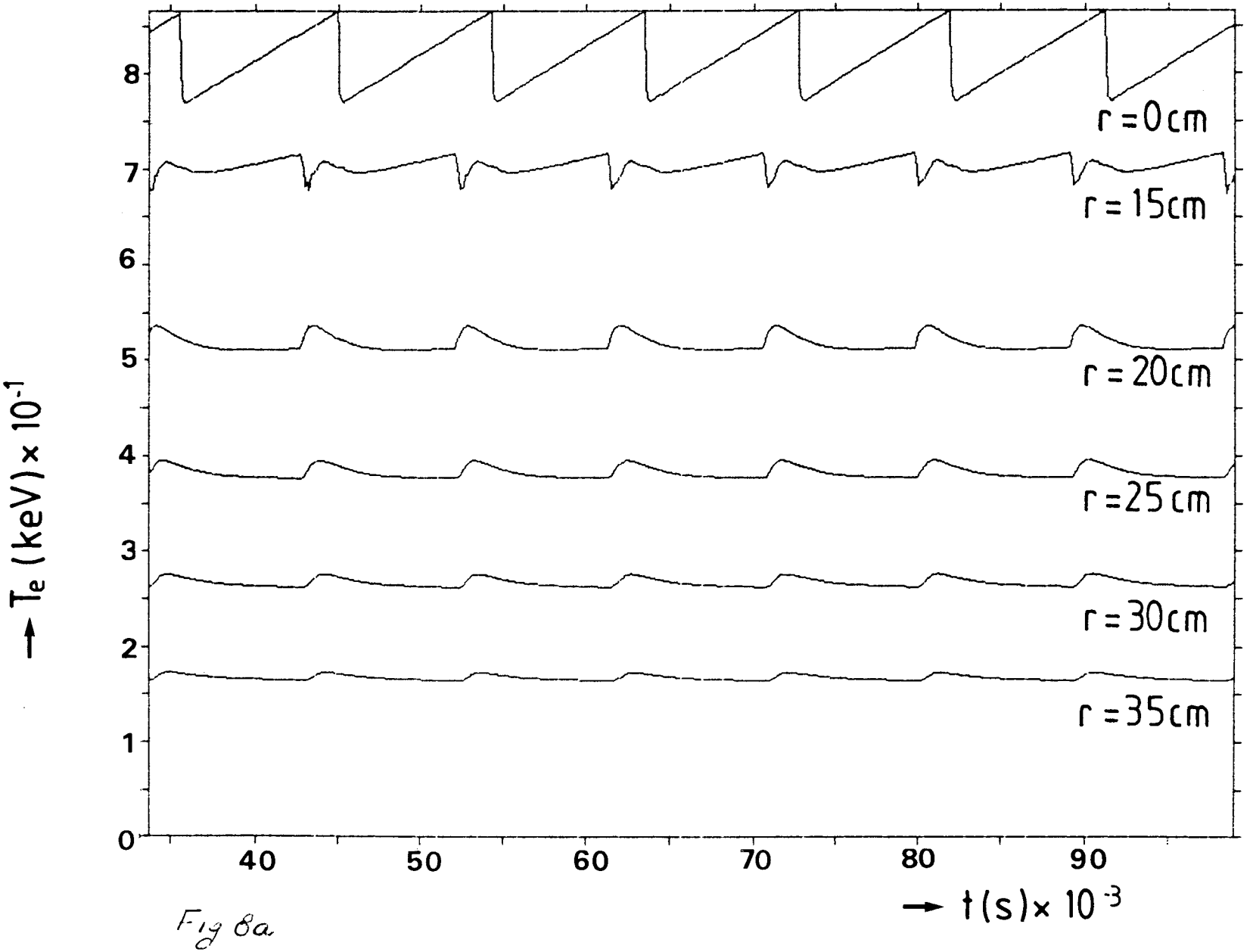
r = 0 cm
r = 15 cm
r = 20 cm
r = 25 cm
r = 30 cm
r = 35 cm
0
1
2
3
4
5
6
7
8
40
50
60
70
80
90
→ T_e (keV) × 10^{-1}
→ t (s) × 10^{-3}

Fig 8a

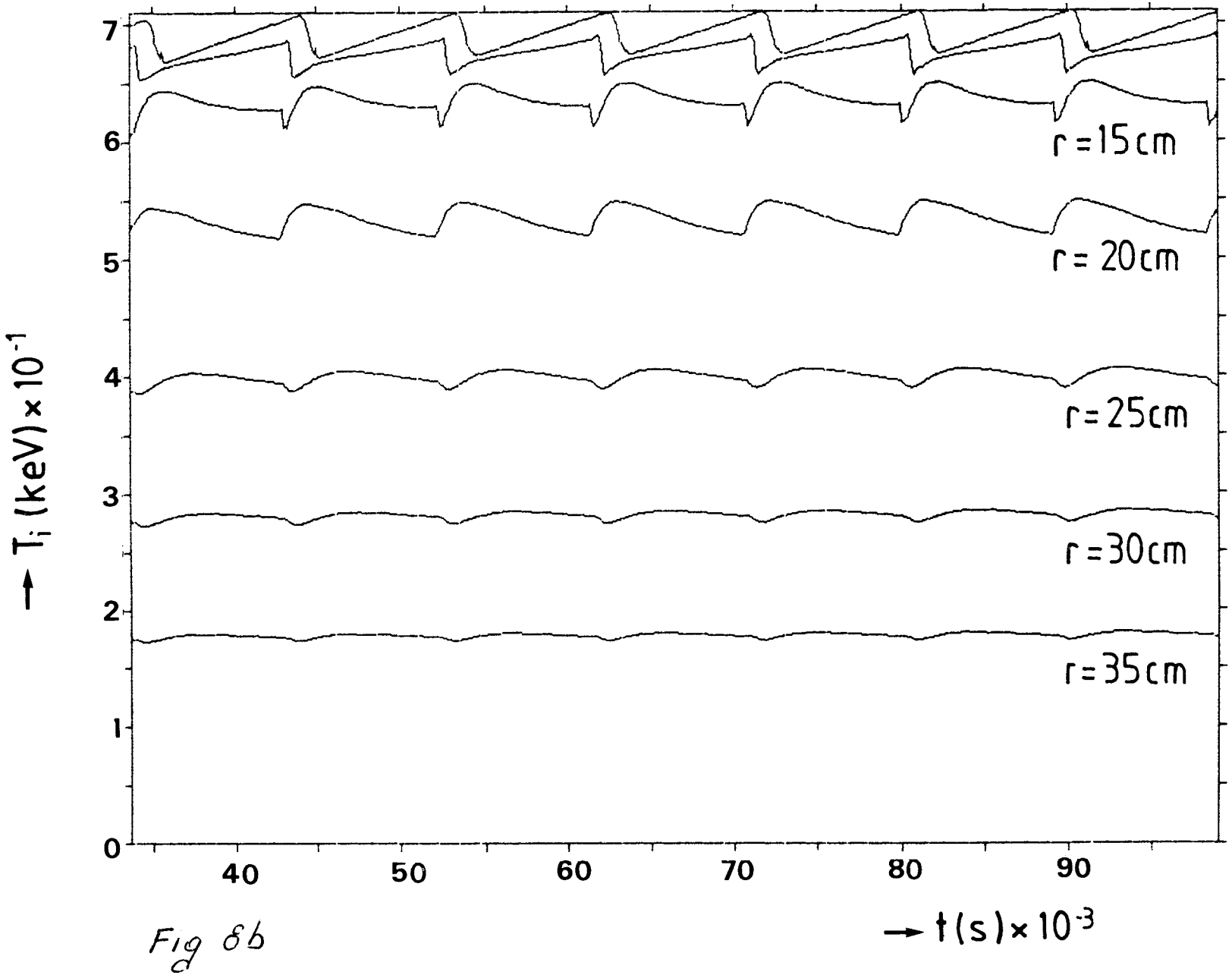
7
6
5
4
3
2
1
0
r = 15 cm
r = 20 cm
r = 25 cm
r = 30 cm
r = 35 cm
40
50
60
70
80
90
→ T_i (keV) × 10^{-1}
→ t (s) × 10^{-3}

Fig 8b